Appendix A

Solutions of exercises

In the following, we present sample solutions together with some further discussions for the theoretical and practical exercises posed in the preceding chapters.

Chapter 2

Exercise 2.1 For the present situation, we determine

$$K(T) \approx (1-T)^{-2}, \qquad |\tau_n^0(U)| \approx \sup_{I_n} |u''| \approx (1-t_n)^{-3},$$

and therefore $h_n \approx (1-T)(1-t_n)^{3/2} N^{-1/2}\,\mathrm{TOL}^{1/2}$. This yields

$$\begin{aligned} N \;=\; \sum_{n=1}^{N} h_n h_n^{-1} \;&\approx\; N^{1/2}(1-T)^{-1}\mathrm{TOL}^{-1/2} \sum_{n=1}^{N} h_n (1-t_n)^{-3/2} \\ &\approx\; N^{1/2}(1-T)^{-3/2}\mathrm{TOL}^{-1/2}, \end{aligned}$$

and, finally, $N \approx (1-T)^{-3}\mathrm{TOL}^{-1}$.

Exercise 2.2 This time, we have $\rho_n \approx \sup_{I_n} |u'| \approx (1-t_n)^{-2}$,

$$\omega_n = \int_{I_n} |z'|\, dt = 2(1-T)^{-2} \int_{I_n} (1-t)\, dt \;\approx\; h_n(1-t_n)(1-T)^{-2},$$

and, analogously to Exercise 2.1, $h_n \approx (1-t_n)^{1/2}(1-T)N^{-1/2}\mathrm{TOL}^{1/2}$. Thus,

$$\begin{aligned} N \;=\; \sum_{n=1}^{N} h_n h_n^{-1} \;&\approx\; N^{1/2}(1-T)^{-1}\mathrm{TOL}^{-1/2} \sum_{n=1}^{N} h_n (1-t_n)^{-1/2} \\ &\approx\; N^{1/2}(1-T)^{-1}\mathrm{TOL}^{-1/2}, \end{aligned}$$

and, finally, $N \approx (1-T)^{-2}\mathrm{TOL}^{-1}$.

Exercise 2.3 For the cG(1) method the dual problem in variational form looks similar to that for the dG(0) method, but without the jump terms:

$$\int_I (\varphi, -z' - B^* z)\, dt + (\varphi(T), z(T)) = (\varphi(T), e_N \|e_N\|^{-1}).$$

Take $\varphi := e$, use integration by parts and Galerkin orthogonality, to obtain

$$\begin{aligned}\|e_N\| &= \int_I (e, -z' - B^* z)\, dt + (e(T), z(T)) = \int_I (e' - Be, z)\, dt + (e(0), z(0)) \\ &= \int_I (e' - f(u) + f(U), z)\, dt = \int_I (f(U) - \overline{f(U)}, z - \bar{z})\, dt,\end{aligned}$$

where $\overline{f(U)}$ denotes the interval-wise mean value of $f(U)$. From this, we obtain

$$\|e_N\| \le c_I \sum_{n=1}^{N} h_n \left(\sup_{I_n} \|f(U) - \overline{f(U)}\| \right) \left(\int_{I_n} \|z'\|\, ds \right) =: c_I \sum_{n=1}^{N} h_n \rho_n \omega_n.$$

Exercise 2.4 (practical exercise) The actually computed relative error $|u(T) - U(T)|/|u(T)$ is compared in Figure A.1 for two different end times $T = 0.95$ and $T = 0.999$, and global refinement as well as the mesh-width formulas used in Exercises 2.1 and 2.2. All three choices lead to an error that is proportional to N^{-1}, for all values of the end time T.

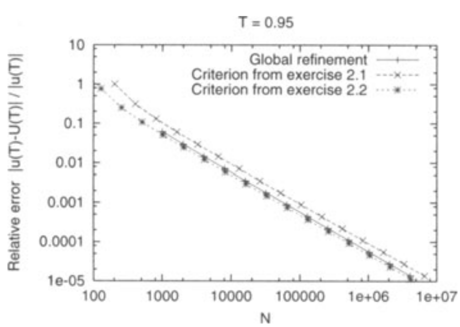

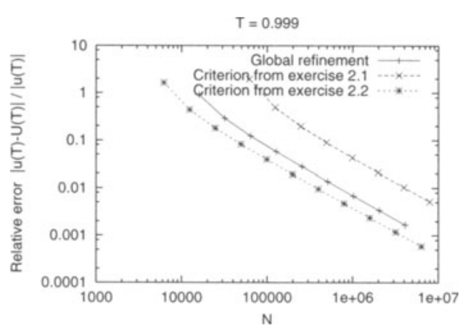

Figure A.1: *Error for various mesh width choices, for end times* $T = 0.95$ *(left) and* $T = 0.999$ *(right).*

Comparing the mesh-width criteria against each other shows that the implicit mesh choice strategy developed from the finite difference point of view is even worse than a globally uniform mesh. On the other hand, the strategy based on the finite element formulation is better than global refinement, with a small but growing margin for end times that are not too close to the critical value $t = 1$. The results do not significantly change if the truncation error and the residuals are approximated numerically, instead of using knowledge of the exact solution as in Exercises 2.1 and 2.2.

If the mesh-width formulas are to be used as stopping criteria, then the actually computed error should not be too far away from the prescribed tolerance for which the respective mesh was made. The left panel of Figure A.2 shows that for the criterion used in Exercise 2.2, these values coincide very well, while the criterion used in Exercise 2.1 produces an error that is actually much better than the prescribed tolerance. This, of course, is due to the fact that in its derivation we have used the worst-case stability constant $K(T)$ rather then the temporally varying dual solution. This overestimation becomes worse as $T \to 1$, and using the tolerance in the mesh choice formula as a stopping criterion will lead to much unnecessary numerical work.

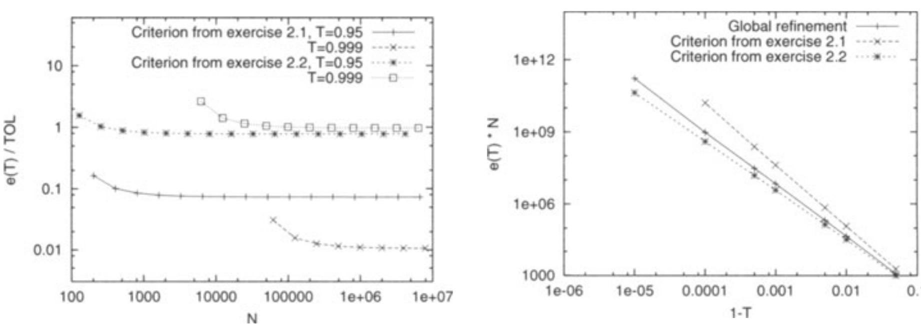

Figure A.2: *Ratio of true (computed) error and prescribed tolerance (left); error* $e(T)N$ *as a function of* $1-T$ *(right).*

In order to check the behavior of the errors as $T \to 1$, we show the behavior of $e(T)\cdot N$ in the right panel of Figure A.2 as a function of $1-T$. The theoretical predictions that $e(T)\cdot N$ be proportional to $|\log(1-T)|(1-T)^{-2}$ (uniform mesh), $(1-T)^{-3}$ (mesh choice after Exercise 2.1), or $(1-T)^{-2}$ (mesh choice after Exercise 2.2) are well confirmed. Compared to global refinement, adaptive mesh refinement thus only gains if we move T very close to 1, for this simple model example.

As a final comparison, Figure A.3 shows the errors at the end time when using the second order cG(1) method with global refinement, and the first order dG(0) method with the optimal mesh width strategy as used in Exercise 2.2. The superiority of the former is striking, in particular as the numerical effort is not much higher. Optimal mesh choice would further improve this method.

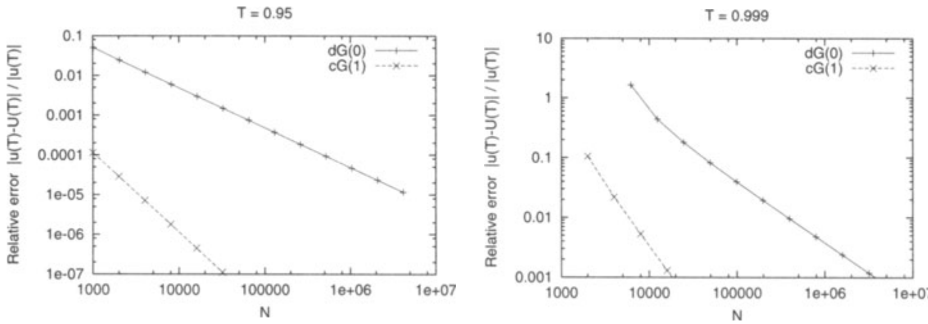

Figure A.3: *Comparison of the cG(1) and the dG(0) method for* $T = 0.95$ *and* $T = 0.999$.

Chapter 3

Exercise 3.1 The approach based on energy error estimates for primal and dual solutions is attractive since such estimates are well known and provide a high degree of accuracy. However, consider the point evaluation of the derivative error

$$J(e) = \partial_1 e(a), \quad a \in \Omega.$$

On uniformly refined meshes, there holds $|J(e)| = \mathcal{O}(h)$, but for $u \in H^2(\Omega)$, and for the singular dual solution z, we only have

$$\|\nabla e\| = \mathcal{O}(h), \quad \|\nabla e^*\| = \mathcal{O}(h^{-1}).$$

On the other hand, on 'optimally' refined meshes,

$$|J(e)| = \mathcal{O}(\mathrm{TOL}),$$

and

$$\|\nabla e\| = \mathcal{O}(\mathrm{TOL}^{1/2}), \quad \|\nabla e^*\| = \mathcal{O}(1).$$

In both cases the energy-norm-error-based estimate is of sub-optimal order. Note that we also cannot extract refinement indicators from the estimate, since it cannot be localizes, i.e., the estimate

$$(\nabla e, \nabla e^*) \le \sum_{K \in \mathbb{T}_h} h_K \|\nabla^2 u\|_K h_K \|\nabla^2 z\|_K$$

does not hold.

Exercise 3.2 The basic idea is to first derive an estimate for the point error at an arbitrary but fixed point a, and later try to use a priori estimates that remove all references to this particular point. For an arbitrary point $a \in \Omega$, use the output functional

$$J_\varepsilon(e) := |B_\varepsilon(a)|^{-1} \int_{B_\varepsilon(a)} e\, dx,$$

with $\varepsilon = \mathrm{TOL}$, which results in

$$|e(a)| \le |J_\varepsilon(e)| + \mathcal{O}(\mathrm{TOL}).$$

For the solution (regularized Green function) of the corresponding dual problem

$$-\Delta z = \delta_\varepsilon^a \quad \text{in } \Omega, \qquad z_{|\partial\Omega} = 0,$$

with $\delta_\varepsilon^a(x) \equiv |B_\varepsilon(a)|^{-1}$ for $x \in B_\varepsilon(a)$, and $\delta_\varepsilon^a \equiv 0$ elsewhere, we have the a priori bound (see, e.g., Ciarlet [46])

$$\|r\nabla^2 z\| \le c\|r^{-1}\| \le c|\log(\mathrm{TOL})|^{1/2},$$

where $r(x) := (|x-a|^2 + \varepsilon^2)^{1/2}$. Note that the last result does not contain references to the point a any more. Now, we estimate as follows:

$$\begin{aligned}
|J_\varepsilon(e)| &\le c_I \sum_{K\in\mathbb{T}_h} h_K^2 \rho_K \|\nabla^2 z\|_K \\
&\le c_I \Big(\sum_{K\in\mathbb{T}_h} h_K^4 \rho_K^2 r_K^{-2} \Big)^{1/2} \Big(\sum_{K\in\mathbb{T}_h} r_K^2 \|\nabla^2 z\|_K^2 \Big)^{1/2} \\
&\le c c_I \max_{K\in\mathbb{T}_h} \{h_K \rho_K\} \|r^{-1}\|\, \|r\nabla^2 z\| \le c c_I |\log(\mathrm{TOL})| \max_{K\in\mathbb{T}_h} \{h_K \rho_K\}.
\end{aligned}$$

Hence, the refinement criterion

$$h_K \rho_K \le \frac{\mathrm{TOL}}{c c_I |\log(\mathrm{TOL})|}$$

yields the required accuracy for the L^∞-norm error.

Exercise 3.3 (practical exercise) a) Figure A.4 shows two optimal meshes generated by the weighted error estimator for the functionals $J(u) = u(a)$ and $J(u) = \partial_1 u(a)$, respectively, with $a = (0.75, 0.75)$. Figure A.5 shows the quality of error estimation on a sequence of these meshes, where for the evaluation of the error representation the dual solution was approximated by piecewise quadratic finite elements. As can be seen, the error is estimated very well.

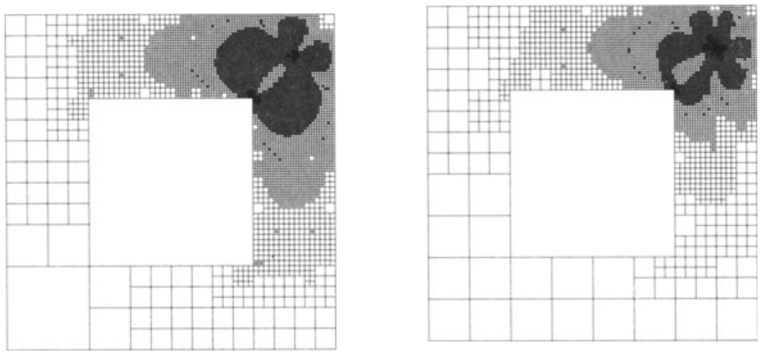

Figure A.4: *Meshes after 7 refinement cycles for the point value* $u(a)$ *(left) and the point derivative* $\partial_1 u(a)$ *(right).*

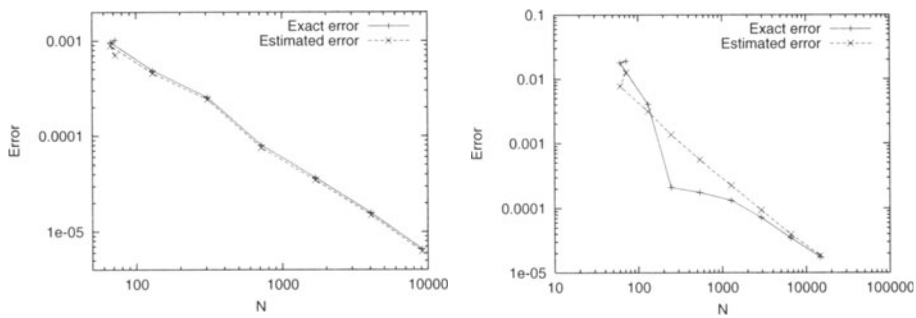

Figure A.5: *Quality of error estimates for the point value* $u(a)$ *(left) and the point derivative* $\partial_1 u(a)$ *(right).*

b) For the point value evaluation $J(u) = u(a)$, the convergence behavior of the error is shown in Figure A.6 for the following refinement criteria:

- Global refinement.
- Edge residuals: We drop the cell residual term from the error representation formula, and remove the weights involving the dual solution by assuming that there exists an a priori stability estimate for its second derivatives. We are then left with the following cell-wise term: $\eta_K = h_K^{1/2} \|[\partial_n u_h]\|_{\partial K}$.
- Weighted edge residuals: We replace the weights involving the dual solution by an a priori guess on each cell. Since for the point value, $\nabla^2 z$ decays as r^{-2}, where $r = |x - a|$, we take as indicator for refinement the expression $\eta_K = h_K^{1/2} \|[\partial_n u_h]\|_{\partial K} r_K^{-2}$.

- The full dual weighted error estimator η_ω .

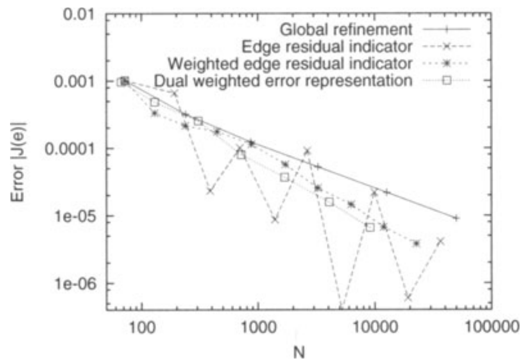

Figure A.6: *Comparison of various refinement criteria for the computation of the point value* $u(a)$.

As can be seen from the figure, a posteriori error indicators do a much better job than global refinement. Using the guessed weight is almost as good as the full weighted error estimator; the difference between the two can probably be attributed to the fact that the weight r^{-2} does not 'see' the singularities of the dual solution at the reentrant corners of the domain, in contrast to the numerically computed approximation

The original edge residual indicator without weights displays a rather irregular behavior. The sign of the error is changing multiply, and the error grows at several refinement steps. The computed values are here, as opposed to the other criteria, not suitable for extrapolation.

Chapter 4

Exercise 4.1 Let N_{old} be the old number of cells, and X and Y the fractions of cells to be refined and coarsened, respectively. Under (bisection-type) refinement, each cell is replaced by 2^d cells, while coarsening merges 2^d cells into one. All other cells remain as they are. The new number of cells is thus

$$N_{\text{new}} = (1 - X - Y + 2^d X + 2^{-d} Y) N_{\text{old}}.$$

a) In order to approximately double the number of cells, we have to choose fractions $0 \le X, Y \le 1, X + Y \le 1$, such that $1 - X - Y + 2^d X + 2^{-d} Y \approx 2$. In 2-D, $X = \frac{1}{3} + \frac{1}{4} Y$ solves this.

b) To keep the number of cells roughly constant, $1 - X - Y + 2^d X + 2^{-d} Y \approx 2$ has to hold. In 2-D, the solution of this equation is $X = \frac{1}{4} Y$.

It should be noted that a cell can only then be coarsened if all its child cells are marked for coarsening. In practice, marking a fraction Y of all cells for coarsening will therefore yield much less cells that will actually be unrefined. Thus, the computations above are only an indication for N_{new}.

Exercise 4.2 The proof of the cell-wise interpolation estimate

$$\|\nabla(u-I_h u)\|_K \le c_I h_K \|\nabla^2 u\|_K$$

via the 'Bramble-Hilbert lemma' combines an abstract functional analytic result of the type of the Poincaré inequality with a scaling argument (see, e.g., Ciarlet [46]). Suppose for simplicity that the mesh is rectangular.

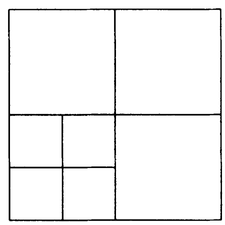

Figure A.7: *Rectangular cell patch with hanging nodes.*

The cell K belongs to a patch $\tilde{K}$ of cells sharing with K the hanging nodes (see Figure A.7), i.e., the interpolation $I_h u$ is well defined by $u_{|\tilde{K}}$. The cell patch $\tilde{K}$ of width h_K is mapped by an affine mapping onto a reference domain $\tilde{K}_1$ of width one. Let I_1 denote the generic analogue of the interpolation operator I_h on $\tilde{K}_1$. With this notation, we consider the functional

$$F(u) := \|\nabla(u-I_1 u)\|_{K_1},$$

which is well defined on the Sobolev space $H^2(\tilde{K}_1)$. It has the following three properties:

$$\begin{aligned} |F(u)| &\le c\,\|u\|_{H^2(\tilde{K}_1)}, && \text{(boundedness)} \\ |F(u+v)| &\le |F(u)| + |F(v)|, && \text{(subadditivity)} \\ F(q) &= 0, \quad q \in P_1(\tilde{K}_1). && \text{(orthogonality)} \end{aligned}$$

The first one follows from the estimate

$$\|\nabla(u-I_h u)\|_{K_1} \le \|\nabla u\|_{K_1} + c\|u\|_{L^\infty(\tilde{K}_1)}$$

which is a consequence of the definition of $I_h u$ and the equivalence of norms on finite dimensional vector spaces, together with the usual Sobolev inequality

$$\|u\|_{L^\infty(\tilde{K}_1)} \le c\|u\|_{H^2(\tilde{K}_1)}.$$

The second one is obvious and the third one follows from the property $I_h u = u$ for $u \in P_1(K_1)$. Then, the abstract Bramble-Hilbert lemma implies that there holds

$$|F(u)| \leq \hat{c}\,\|\nabla^2 u\|_{\tilde{K}_1},$$

with a constant $\hat{c}$ depending only on the shape of the reference domain $\tilde{K}_1$. The asserted estimate then follows by a standard scaling argument from $\tilde{K}_1$ to $\tilde{K}$.

Exercise 4.3 (practical exercise) In FigureA.8, the error in the target functional $J(u) = \partial_1 u(a)$ is shown for both global refinement and refinement by the weighted error estimator. Obviously, the introduction of hanging nodes does not destroy the better convergence of the adapted meshes. In this case, one of the four cells adjacent to the evaluation point even has a hanging node on all levels of refinement. Yet, the results are better than as could be obtained on globally refined meshes with their regular mesh structure in the vicinity of the evaluation point. Removing this single hanging node produces better results but with a less smooth convergence behavior. It seems that also on locally refined meshes the *super-approximation* effect for the approximation of $\partial_1 u(a)$ is picked up, provided that the mesh is uniform in a small neighborhood of the point a.

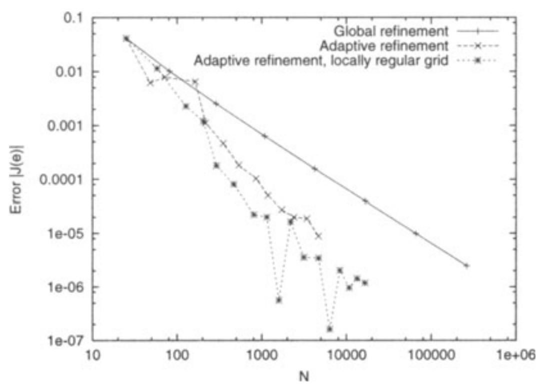

Figure A.8: *Error in the functional* $\partial_1 u(a)$ *for global refinement and refinement by the weighted error estimator.*

Chapter 5

Exercise 5.1 Choosing $\varepsilon = \mathrm{TOL}^{1/2}$ is actually possible here, since the difference between the point value and the integral mean over a domain which is symmetric to this point is quadratic in the diameter of this domain. A computation analogous to the one at the beginning of Chapter 5 shows that for general regularization parameters ε, the minimal mesh width satisfies $h_{\min}^2 = \varepsilon^{3/2} TOL$. Thus, for $\varepsilon = TOL$, we have $h_{\min} = TOL^{5/4}$, while for $\varepsilon = TOL^{1/2}$, there holds $h_{\min} = TOL^{7/8}$. Since each refinement step reduces the mesh width by a factor two (starting from an assumed coarsest cell of diameter ≈ 1), the number of refinement steps necessary to reach $h_{\min}$ is $L = -\log_2 h_{\min}$. Thus, for the choices of ε, we get

$$L \approx \frac{5}{4}\frac{|\log TOL|}{|\log 2|}, \qquad \text{and} \qquad L \approx \frac{7}{8}\frac{|\log TOL|}{|\log 2|},$$

respectively. Therefore, the choice $\varepsilon = TOL^{1/2}$ reduces the necessary number of refinement steps by 30 per cent. Note that this choice of ε is not possible if the point of evaluation is closer to the boundary than TOL.

Exercise 5.2 Any reasonable choice for ψ_h has to satisfy the following criteria:
(i) it must be from the discretization space V_h;
(ii) it should be locally constructible from z;
(iii) it should satisfy a local interpolation property such as

$$\|z - \psi_h\|_K \le c h_K^2 \|\nabla^2 z\|_K.$$

On the other hand, we would like to choose ψ_h in such a way that the cell terms in the error representation are small compared to the edge terms. For simplicity, assume that the mesh consists solely of rectangles. Then $\Delta u_h = 0$, and the cell terms have the form $(f, z - \psi_h)_K$. Ideally, we would then like to choose ψ such that it interpolates z and that the mean value of $z - \psi_h$ is zero. In this case, the cell-wise mean value $\bar{f}$ of f would be orthogonal to the weights, and we could estimate

$$(f, z - \bar{z})_K = (f - \bar{f}, z - \bar{z})_K \le \|f - \bar{f}\|_K \|z - \bar{z}\| \le c h_K^3 \|\nabla f\|_K \|\nabla^2 z\|_K,$$

making the term of higher order than the edge term. Unfortunately, this construction is not possible: if ψ_h shall interpolate z and be in V_h, then we do not have a degree of freedom left on each cell to satisfy the mean value property.

However, this construction is possible: let $\tilde{K}$ be a patch of four cells, then set $\psi_h(a_i) = z(a_i)$ on each of the eight vertices a_i at the boundary of $\tilde{K}$, and determine the remaining degree of freedom at the center vertex such that $\int_{\tilde{K}} (z - \psi_h)\, dx = 0$. This choice of ψ_h satisfies all the criteria listed above. The interpolation estimates and estimates for $f - \bar{f}$ now hold on $\tilde{K}$ instead if K, but as this is only an $\mathcal{O}(h)$ environment, this does not disturb us.

Exercise 5.3 (practical exercise) a) Figure A.9 shows the numerically computed approximation of the second derivatives for grids generated for the two functionals given in the exercise. Initially, the formula gives cell-wise constant values, but since this is a quantity that leads to poorly visible graphics, we generate a function where the value at each vertex is the mean value of the cell-wise quantities on the adjacent cells.

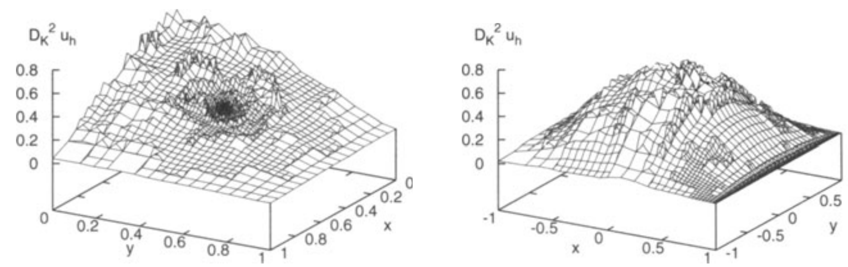

Figure A.9: $D_K^2 u_h$ *on parts of optimal meshes generated by the dual weighted error estimator for* $J(u) = \partial_1 u(a)$ *(left) and* $J(u) = \int_{-1}^{1} \partial_n u(1,y)dy$ *(right).*

It can be seen that the result is a relatively smooth function except for those cells with hanging nodes. At these, the computed value is larger than on patches of uniform grids, and the ratio with the value of the second derivative of the exact solution does not converge to one. However, computing on a sequence of successively finer grids, the maximal value of the approximation to the second derivatives remains bounded for both examples.

b) For the regular solution, the same holds as said above for the quotient of the computed approximation of the second derivative with the asymptotic exact second derivatives, shown in Figure A.10. Again, the values remain bounded, but are irregular at cells with hanging nodes.

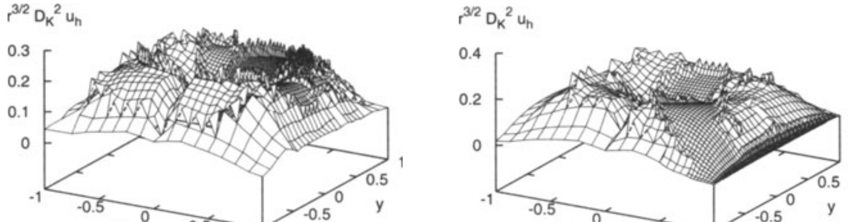

Figure A.10: $\tilde{D}_K^2 u_h$ *on optimal meshes generated by the weighted error estimator for computing* $J(u) = \partial_1 u(a)$ *(left) and* $J(u) = \int_{-1}^{1} \partial_n u(1,y)\, dy$ *(right).*

Chapter 6

Exercise 6.1 For the Burgers equation, the semilinear form and its derivatives are

$$\begin{aligned} A(u)(z) &= \nu(u_x, z_x) + (uu_x, z) - (f, z) \\ A'(u)(w, z) &= \nu(w_x, z_x) + (uw_x, z) + (wu_x, z) \\ A''(u)(\varphi, w, z) &= (\varphi w_x, z) + (w\varphi_x, z) \\ A'''(u)(\psi, \varphi, w, z) &= 0. \end{aligned}$$

The second- and third-order remainder terms are thus

$$\begin{aligned} \mathcal{R}_h^{(2)} &= \int_0^1 \{A''(u_h+se)(e, e, z) - J''(u_h+se)(e, e)\} s\, ds \\ &= \int_0^1 2(ee_x, z)\, s\, ds = (ee_x, z), \\ \mathcal{R}_h^{(3)} &= \tfrac{1}{2} \int_0^1 \{J'''(u_h+se)(e, e, e) - A'''(u_h+se)(e, e, e, z_h+se^*) \\ &\qquad - 3A''(u_h+se)(e, e, e^*)\}\, s(s-1)\, ds \\ &= -3 \int_0^1 (ee_x, e^*)\, s(s-1)\, ds = \tfrac{1}{2}(ee_x, e^*). \end{aligned}$$

Exercise 6.2 Use the output functional

$$J(\varphi) := \tfrac{1}{2}\|u-\varphi\|^2,$$

to obtain $J(u) - J(u_h) = -\frac{1}{2}\|e\|^2$. Its derivatives are

$$J'(v)(w) = (u-v, w), \qquad J''(v)(w, \varphi) = -(w, \varphi).$$

The solution of the corresponding dual problem

$$(\nabla\varphi, \nabla z) = J'(u_h)(\varphi) = (e, \varphi) \quad \forall\varphi,$$

satisfies the a priori bound $\|\nabla^2 z\| \le c_S\|e\|$. This yields the error identity

$$-\tfrac{1}{2}\|e\|^2 = -\rho(u_h)(z - I_h z) + \mathcal{R}_h^{(2)},$$

with the second-order remainder term

$$\mathcal{R}_h^{(2)} = \int_0^1 \{A''(u_h+se)(e, e, z) - J''(u_h+se)(e, e)\} s\, ds = \tfrac{1}{2}\|e\|^2.$$

Now proceed by bringing the remainder term to the left hand side, and using the standard argument to obtain

$$\|e\|^2 = \rho(u_h)(z - I_h z) \le c_I c_S \rho_{L^2}(u_h)\|e\|,$$

with the L^2-norm error estimator $\rho_{L^2}(u_h)$ as defined in Section 3.2. Note that we have actually made use of the remainder term in this example, and that it cannot be neglected here.

Exercise 6.3 (practical exercise) Figure A.11 shows the primal and dual solutions for the mean-value functional.

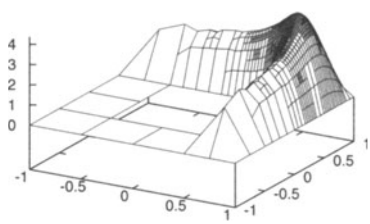

Figure A.11: *Primal and dual solutions for the mean-value functional.*

Figure A.12 shows the ratio of the nonlinearity indicator $\Delta\rho$ and the (second-order error estimate) $(\rho+\rho^*)/2$. In the left graph, this ratio is shown when primal and dual weights are approximated by a patch-wise higher-order interpolation. The result is a rather small value of the nonlinearity indicator, much less than 1 per cent even as we approach the critical eigenvalue $\alpha \approx 72.3$ (see also the solution to exercise 7.4).

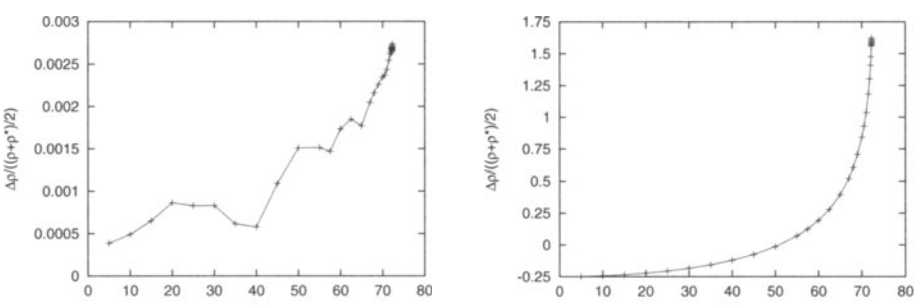

Figure A.12: *Ratio $\Delta\rho/((\rho+\rho^*)/2)$ between the nonlinearity term and the error estimate. Left: Approximation of primal and dual weights by patch-wise biquadratic interpolation. Right: Approximation of the dual weight by a higher-order Ritz projection. Note the difference in scale.*

However, as the right graph of the figure indicates, the above result is misleading: if the dual solution is approximated by a higher-order Ritz projection, then ρ and ρ^* are no more as close together, and $\Delta\rho$ becomes large, especially as we approach the critical eigenvalue. Close to the critical value, the difference between the two residuals becomes larger than the residuals themselves, making the error estimate quite unreliable.

The interpretation of this is that if both primal and dual weights are approximated using a higher-order interpolation, then the approximated residuals $\tilde{\rho}$ and $\tilde{\rho}^*$ are both not particularly close to the exact error, but the effects of approximation shift their values in the same direction, thus canceling out and pretending a small $\Delta\rho$. On the other hand, when replacing z by its biquadratic Ritz projection, ρ is computed to a high accuracy, while ρ^* is still inaccurate because the weights in this term are only obtained by interpolation. Then, the approximation effect in ρ^* is not canceled by that in ρ, and we obtain a large value for $\Delta\rho$.

In effect, the evaluation of $\Delta\rho$ does not tell us very much in this particular example, if we do not take into account the effects of numerically approximating the weights in the residuals.

Chapter 7

Exercise 7.1 We recall the defining equations

$$\begin{aligned} a(u,\psi) &= \lambda\,(u,\psi) \quad \forall \psi \in V, \quad \|u\| = 1, \\ a(u_h,\psi_h) &= \lambda_h\,(u_h,\psi_h) \quad \forall \psi_h \in V_h, \quad \|u_h\| = 1. \end{aligned}$$

Consequently,

$$\begin{aligned} \lambda - \lambda_h &= \tfrac{1}{2}(\lambda-\lambda_h)\{\|u_h\|^2 + \|u\|^2\} \\ &= \tfrac{1}{2}(\lambda-\lambda_h)\{\|u_h\|^2 - 2(u_h,u) + \|u\|^2\} + (\lambda-\lambda_h)(u_h,u) \\ &= \tfrac{1}{2}(\lambda-\lambda_h)\|u-u_h\|^2 + \lambda(u_h,u) - \lambda_h(u_h,u) \\ &= \tfrac{1}{2}(\lambda-\lambda_h)\|u-u_h\|^2 + a(u_h,u) - \lambda_h(u_h,u) \\ &= \tfrac{1}{2}(\lambda-\lambda_h)\|u-u_h\|^2 + \rho(u_h,\lambda_h)(u). \end{aligned}$$

Using Galerkin orthogonality $\rho(u_h,\lambda_h)(\psi_h) = 0,\ \psi_h \in V_h$, the asserted representation follows.

Exercise 7.2 We recall the estimate (7.12) from Proposition 7.3,

$$|\lambda - \lambda_h| \le \eta_\lambda^\omega := \sum_{K\in\mathbb{T}_h} \{\rho_K\omega_K^* + \rho_K^*\omega_K\},$$

$$\begin{aligned}
\rho_K &:= \left(\|R_h\|_K^2 + h_K^{-1}\|r_h\|_{\partial K}^2\right)^{1/2},\\
\rho_K^* &:= \left(\|R_h^*\|_K^2 + h_K^{-1}\|r_h^*\|_{\partial K}^2\right)^{1/2}\\
\omega_K^* &:= \left(\|u^* - I_h u^*\|_K^2 + h_K\|u^* - I_h u^*\|_{\partial K}^2\right)^{1/2},\\
\omega_K &:= \left(\|u - I_h u\|_K^2 + h_K\|u - I_h u\|_{\partial K}^2\right)^{1/2}.
\end{aligned}$$

It remains to estimate the weights ω_K and ω_K^*. By the usual estimates for the nodal interpolations $I_h u$ and $I_h u^*$, we have

$$\omega_K^* \le c_I h_K^2 \|\nabla^2 u^*\|_K, \qquad \omega_K \le c_I h_K^2 \|\nabla^2 u\|_K.$$

This gives us the intermediate result

$$|\lambda - \lambda_h| \le c_I\Big(\sum_{K\in\mathbb{T}_h} h_K^4 \rho_h^2\Big)^{1/2} \|\nabla^2 u^*\| + c_I\Big(\sum_{K\in\mathbb{T}_h} h_K^4 \rho_h^{*2}\Big)^{1/2} \|\nabla^2 u\|.$$

Since u and u^* are eigenfunctions of the operators $\mathcal{A} := -\Delta + b\cdot\nabla$ and $\mathcal{A}^* := -\Delta - b\cdot\nabla$, respectively, there holds

$$\|\nabla^2 u\| + \|\nabla^2 u^*\| \le c_1(\mathcal{A})\left\{\|\mathcal{A}u\| + \|\mathcal{A}^* u^*\|\right\} = c_1(\mathcal{A})|\lambda|\left\{\|u\| + \|u^*\|\right\},$$

with some constant $c_1(\mathcal{A})$. Since $\|u^*\| \le c_2(\mathcal{A})$, the asserted estimate follows.

Exercise 7.3 Let $w(t)$ solve the (nonstationary) *perturbation equation*

$$\partial_t w - \nu\Delta w + \hat{u}\cdot\nabla w + w\cdot\nabla\hat{u} = 0,$$

corresponding to some initial perturbation $w_{|t=0} = w_0$. Taking the scalar product with w, and observing that

$$(\hat{u}\cdot\nabla w, w) = \tfrac{1}{2}(\hat{u}, \nabla w^2) = -\tfrac{1}{2}(\nabla\cdot\hat{u}, w^2)$$

yields

$$\tfrac{1}{2}d_t\|w\|^2 + \nu\|\nabla w\|^2 + (\{\nabla\hat{u}^T - \tfrac{1}{2}\nabla\cdot\hat{u}I\}w, w) = 0, \quad t \ge 0.$$

If now

$$\nu\|\nabla w\|^2 + (\{\nabla\hat{u}^T - \tfrac{1}{2}\nabla\cdot\hat{u}I\}w, w) \ge 0,$$

then integration with respect to t implies

$$\tfrac{1}{2}\|w(t)\|^2 - \tfrac{1}{2}\|w_0\|^2 \le 0,$$

i.e., the L^2 norm of the perturbation $w(t)$ stays bounded. Hence, a sufficient criterion for the L^2 stability of the base solution $\hat{u}$ is that all eigenvalues λ of the following *symmetric* eigenvalue problem in V are nonnegative:

$$-\nu\Delta w + \tfrac{1}{2}\{\nabla\hat{u} + \nabla\hat{u}^T - \nabla\cdot\hat{u}I\}w = \lambda w.$$

Exercise 7.4 (practical exercise) In the left part of Figure A.13, the stability eigenvalue $\lambda_{\min}$ is shown. As the forcing strength α approaches the critical value $\alpha_{\text{crit}} \approx 72.3$, the solution $\hat{u}$ of the base problem $-\Delta\hat{u} - \hat{u}^3 = \alpha$ grows until the smallest eigenvalue of the operator $-\Delta - 3\hat{u}^2$ becomes zero.

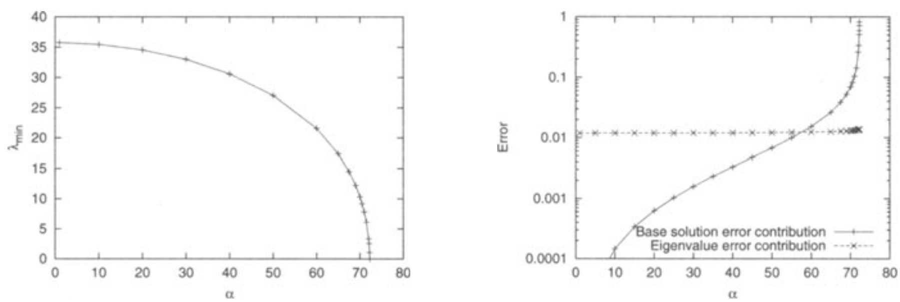

Figure A.13: *Numerically computed stability eigenvalues $\lambda_{\min}$ as function of the forcing strength α (left). Base solution error contribution $\hat{\eta}_\lambda = \frac{1}{2}\hat{\rho} + \frac{1}{2}\hat{\rho}^*$ and eigenvalue approximation error contribution $\eta_\lambda = \frac{1}{2}\rho + \frac{1}{2}\rho^*$ (right).*

For the computation of this stability eigenvalue, we want to use the error representation formula for $\lambda - \lambda_h$, consisting of the terms $\hat{\eta}_\lambda = \frac{1}{2}\hat{\rho} + \frac{1}{2}\hat{\rho}^*$ for the accuracy of the base solution, and $\eta_\lambda = \frac{1}{2}\rho + \frac{1}{2}\rho^*$ for the accuracy of the eigenvalue approximation. Note that $\rho = \rho^*$ for the symmetric problem under consideration here. In the right part of Figure A.13, the sizes of $\hat{\eta}_\lambda$ and η_λ are shown for a fixed, uniformly refined grid with roughly 50,000 cells.

As can be seen from the comparison of the two components of the error estimator, the error due to the approximation of the eigenvalue grows only very moderately as $\alpha \to \alpha_{\text{crit}}$. On the other hand, the error contribution due to the approximation of the base solution becomes very large, eventually to the same order of magnitude as the eigenvalue itself on this particular grid when near to the critical value of α. This then indicates that the present grid is entirely unsuitable for the computation of a stability eigenvalue. It should be noted that for all values of α, the estimated error is indeed relatively close to the true error.

Chapter 8

Exercise 8.1 The Lagrangian for this problem has the form

$$L(u,q,\lambda) = J(u) - A(u)(\lambda) = \tfrac{1}{2}\|u-\bar{u}\|^2 - (\nabla u, \nabla\lambda) - (qu,\lambda) - (f,\lambda).$$

The error estimator for $J(u,q)-J(u_h,q_h) = J(u)-J(u_h)$ reads

$$J(u) - J(u_h) = \tfrac{1}{2}L'(u_h,q_h,\lambda_h)(u-\varphi_h, q-\chi_h, \lambda-\psi_h) + \mathcal{R}_h,$$

for arbitrary test functions $\varphi_h, \chi_h, \psi_h$, and a remainder term $\mathcal{R}_h$ cubic in the errors. Since only one term of the Lagrangian is cubic, the remainder is a multiple of $(e^q e^u, e^\lambda)$. Also, since $q \in \mathbb{R}$, the corresponding test function χ_h is a scalar as well, and we can make the residual term $L'_q(u_h,q_h,\lambda_h)(q-\chi_h)$ to zero by choosing $\chi_h = q$. For the rest of the estimator, we introduce residual and weight terms

$$\begin{aligned}
\rho_K^u &= \big(\|f+\Delta u_h - q_h u_h\|_K^2 + \tfrac{1}{4}h_K^{-1}\|[\partial_n u_h]\|_{\partial K}^2\big)^{1/2},\\
\rho_K^\lambda &= \big(\| -(u_h-\bar{u})+\Delta\lambda_h - q_h\lambda_h\|_K^2 + \tfrac{1}{4}h_K^{-1}\|[\partial_n \lambda_h]\|_{\partial K}^2\big)^{1/2},\\
\omega_K^u &= \big(\|u-I_h u\|_K^2 + h_K\|u-I_h u\|_{\partial K}^2\big)^{1/2},\\
\omega_K^\lambda &= \big(\|\lambda-I_h \lambda\|_K^2 + h_K\|\lambda-I_h \lambda\|_{\partial K}^2\big)^{1/2},
\end{aligned}$$

to obtain

$$J(u) - J(u_h) = \sum_{K\in\mathbb{T}_h} \{\rho_K^u\omega_K^\lambda + \rho_K^\lambda\omega_K^u\}.$$

Exercise 8.2 The Lagrangian for this problem reads

$$L(u,\lambda,z) = J(u) - A(u)(z) = \tfrac{1}{2}(u-1,1)^2 - (\nabla u, \nabla z) + \lambda(u,z).$$

From this, we obtain the optimality conditions determining a solution to the constrained optimization problem:

$$\begin{aligned}
L'_u(u,\lambda,z)(\varphi) &= (u-1,1)(\varphi,1) - (\nabla\varphi,\nabla z) + \lambda(\varphi,z) = 0,\\
L'_\lambda(u,\lambda,z)(\mu) &= (u,z) = 0,\\
L'_z(u,\lambda,z)(\psi) &= -(\nabla u,\nabla\psi) + \lambda(u,\psi) = 0,
\end{aligned}$$

for all test functions $\{\varphi,\mu,\psi\}$. In strong form, the first and last equations read

$$-\Delta u - \lambda u = 0, \quad -\Delta z - \lambda z = (u-1,1).$$

The first determines the eigenvalue λ and the eigenfunction u up to a multiplicative constant. Since the second optimality condition above requires that z has no component in direction of u, this removes the kernel of the operator $-\Delta-\lambda$, using the assumption of simplicity of this eigenvalue. Furthermore, the adjoint equation has a solution only if the right hand side (which is a constant) is in the range of the operator, $\mathcal{R}(-\Delta-\lambda) = \mathcal{N}(-\Delta-\lambda)^\perp = \{u\}^\perp$; this condition is only satisfied if either the constant right hand side is zero, or if u has mean value zero. Since it is known that the lowest eigenfunction of the Laplacian does not change its sign, the second case cannot occur. In the first case, u is normalized, and the solution of the adjoint equation is necessarily $z \equiv 0$. Since in the error representation formula all terms contain z multiplicatively, the error is zero, for every grid chosen.

The reason for this surprising behavior is that we have set out to control the error in the functional $J(u) = \frac{1}{2}\{(u,1)-1\}^2$. For the exact minimizer, $J(u) = 0$. On the other hand, we can find discrete eigenvalue/eigenvector pairs on *every* grid, and can normalize the eigenvector to $(u_h, 1) = 1$. So $J(u_h)$ can be made equal to zero as well on each grid, making $J(u) - J(u_h) = 0$. Thus, the error estimator only tells us that we can make the error in this quantity to zero on every grid.

Exercise 8.3 (practical exercise) In Figure A.14, two grids generated by an energy-norm error estimator and the weighted error estimator are compared. It is obvious that the latter takes into account that the solution needs to be represented accurately at the observation boundary Γ_O at the right, while the energy-norm error estimator only sees the structure of the primal solution, in particular near the control boundary Γ_C at the bottom, and at the corners next to it. Primal and adjoint solutions obtained on the second grid are shown in Figure A.15.

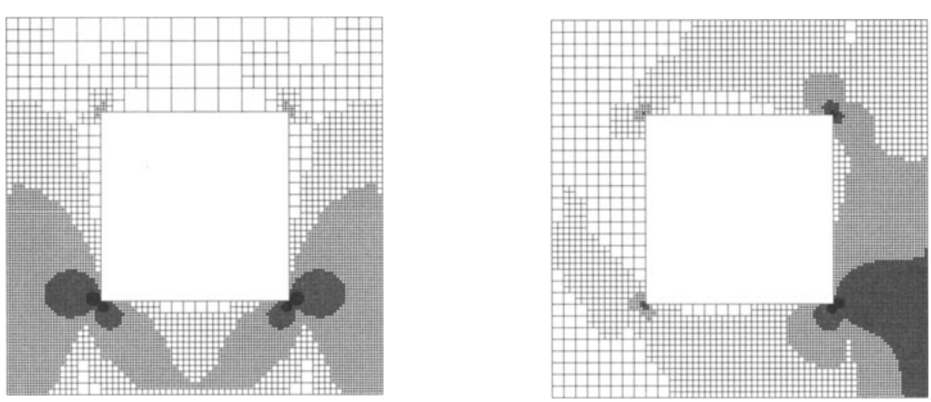

Figure A.14: *Grids generated by an energy-norm error estimator for the primal solution (left) and by the weighted error estimator (right), with approximately 9,000 cells each. Control boundary at the bottom, observation at the right.*

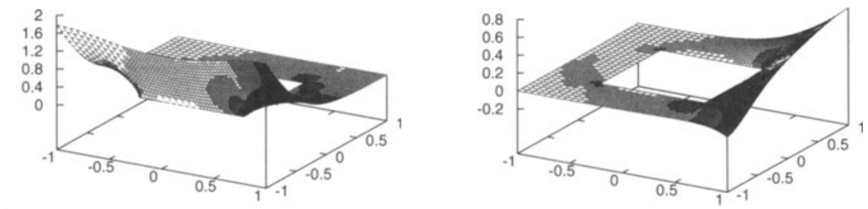

Figure A.15: *Primal (left) and adjoint solution (right) computed on the right grid of Figure A.14.*

Finally, we check the quality of the generated meshes. In the left part of Figure A.16, the error in the optimal control parameter, $|q - q_h|$, is shown. Obviously, the grids generated by the weighted error estimator are not as efficient in reducing this error as the energy-norm error estimator. However, this should not surprise us, since the weighted estimator used the natural output functional, $J(u) = \frac{1}{2}\|u - \bar{u}\|^2_{\Gamma_O}$, rather than a functional involving the control parameter q. On the other hand, the right part of Figure A.16 shows clearly that the meshes generated by the DWR method are superior in reducing the error in the functional for which it was made. Making the DWR method superior also for the error in q would require to solve a dual problem with a different output functional.

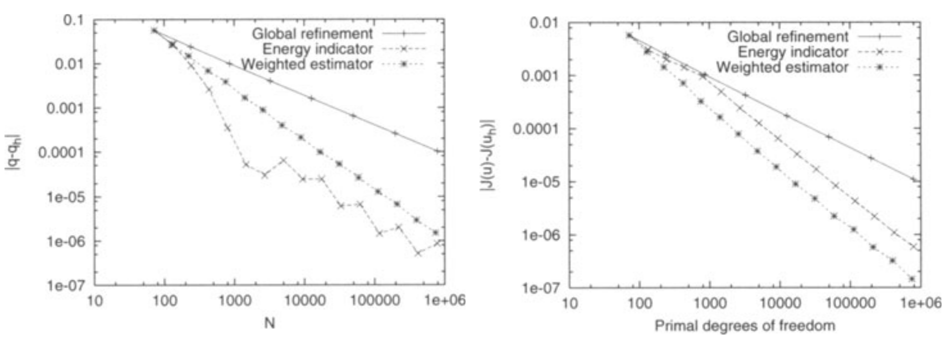

Figure A.16: *Error in the control parameter q (left) and in the misfit functional J (right) for different mesh refinement criteria.*

Chapter 9

Exercise 9.1 Since trial functions are piecewise linear and continuous in time, while test functions are piecewise constant, the discretized problem decouples into a system of equations for each time-step:

$$
\begin{aligned}
(u_h^n - u_h^{n-1}, \psi_h)_\Omega + \tfrac{1}{2}k_n(\nabla(u_h^n + u_h^{n-1}), \nabla\psi_h)_\Omega &= (f, \psi_h)_{\Omega\times I_n} \qquad \forall \psi_h \in V_h^n, \\
(u_h^0, \psi_h)_\Omega &= (u^0, \psi_h)_\Omega \qquad \forall \psi_h \in V_h^n,
\end{aligned}
$$

Thus, the error estimator has the form

$$
\begin{aligned}
J(e) = \sum_{n=1}^{N} \sum_{K\in T_h^n} &(f - \partial_t u_h + \Delta u_h, z - z_h)_{K\times I_n} + \tfrac{1}{2}([\partial_n u_h], z - z_h)_{\partial K\times I_n} \\
&+ (u_h^0 - u^0, (z - z_h)_{|t=0})_\Omega\, .
\end{aligned}
$$

For the end-time error, we take the scalar products of residuals and weights apart and use a priori estimates for $z - z_h$ to eliminate the dual solution. Since the test space from which z_h is taken is the same as for the dG(0) method, the same steps as in Section 9.2 can be used to accomplish this.

Exercise 9.2 The given formulation differs from the one used in Section 9.3 only in the way the velocity equation $\partial_t w = v$ is enforced: instead of L^2-scalar products with test functions, we use the Dirichlet form. Thus, the only difference to the estimator given in the main text is the form of the residual of the first equation, which now reads

$$
R_h^w = -\Delta(\partial_t w_h - v_h),
$$

and the addition of another term $(r_h^w, z^w - \varphi_h^w)_{\partial K\times I_n}$ with jump residuals

$$
r^w_{h\,|\Gamma\times I_n} = \begin{cases} -\tfrac{1}{2}[\partial_n(\partial_t w_h - v_h)] & \text{if } \Gamma \not\subset \partial\Omega, \\ 0 & \text{otherwise.} \end{cases}
$$

Exercise 9.3 (practical exercise) Since the (negative) Laplace operator possesses a complete orthonormal basis $\{v_i\}_{i=1}^\infty$ of eigenvectors with corresponding (positive) eigenvalues λ_i, the solution of the heat equation is given by

$$
u = \sum_{i=1}^{\infty} \lambda_i^{-1}(1, w_i)_\Omega \left(1 - e^{-\lambda_i t}\right) w_i.
$$

As the lowest eigenfunction of the Laplace operator, w_1, is the only one that does not change sign, and since λ_1 is the smallest eigenvalue, the respective coefficient is the largest for this given right-hand side. Thus, the dynamics of the solution can be well approximated by only considering this particular mode, and the choice of a fixed grid is justified if we are not interested in the initial behavior.

Consequently, if h is small enough (e.g., $h^2 = \mathcal{O}(k)$), we have for the end-time error due to equation (9.18):

$$\|e^{N-}\|^2 \leq c \sum_{n=1}^{N} \sigma_n^{-1} \tau_n^{-1} k_n^2 (\rho_k^n)^2,$$

with the total time residual $(\rho_k^n)^2 := \sum_{K \in \mathbb{T}_h} (\rho_{K,k}^n)^2$. Using the definition of σ, neglecting the effect of τ, and approximating the residual by the first mode, we obtain

$$\|e^{N-}\|^2 \leq c \sum_{n=1}^{N} e^{-\lambda_1 T} e^{\lambda_1 t_n} k_n^3 e^{-2\lambda_1 t_n} = c \sum_{n=1}^{N} e^{-\lambda_1 T} e^{-\lambda_1 t_n} k_n^3.$$

An error-balancing strategy would thus choose

$$k_n \propto \frac{TOL^2}{N} e^{\lambda_1 T/3} e^{\lambda_1 t_n/3},$$

resulting in a complexity of $N \propto TOL^{-1} e^{-\lambda_1 T/2}$. The difference to the example shown in Section 9.2, where k_n decreases towards the end time, stems from the fact that there $\|\partial_t u(t)\| = \mathcal{O}(1)$.

Chapter 10

Exercise 10.1 Starting at the present iterate u_h^k, the next Newton update direction δu_h^k is computed using the equation

$$a'(u_h^k)(\delta u_h^k, \psi_h) = -a(u_h^k)(\psi_h) \qquad \forall \psi_h \in V_h.$$

Since the semilinear form $a(\cdot)(\cdot)$ is not differentiable, we approximate the above equation by

$$\tilde{a}'(u_h^k)(\delta u_h^k, \psi_h) = -a(u_h^k)(\psi_h) \qquad \forall \psi_h \in V_h,$$

with $\tilde{a}'(u_h^k)(\delta u_h^k, \psi_h) = (\tilde{C}'(\varepsilon(u_h^k))\delta u_h^k, \varepsilon(\psi_h))$, and $\tilde{C}'$ as defined in (10.12).

The solvability of the Newton update equation can be shown in the same way as that of the linear elastic equations. For this, note that there the bilinear form reads $(2\mu\varepsilon(u)^D + \kappa \operatorname{tr}(\varepsilon(u))I, \varepsilon(\psi))$, where here, using the definition of $\tilde{C}'$, we only have to replace the coefficient μ by the spatially varying coefficient

$$\tilde{\mu} = \begin{cases} \mu I & \text{where } |\tau^D| = |\varepsilon(u_h^k)^D| \leq \sigma_0, \\ \frac{1}{2}\frac{\sigma_0}{|\tau^D|}\left\{\delta_{ij}\delta_{kl} - \frac{\tau_{ij}^D \tau_{kl}^D}{|\tau^D|^2}\right\} & \text{where } |\tau^D| = |\varepsilon(u_h^k)^D| > \sigma_0. \end{cases}$$

It thus remains to show that the fourth order tensor in the second line is positive definite, i.e.

$$\varepsilon_{ij}^D\Big\{\delta_{ij}\delta_{kl} - \frac{\tau_{ij}^D\tau_{kl}^D}{|\tau^D|^2}\Big\}\varepsilon_{kl}^D \geq 0,$$

for all ε^D. This, however, is obvious.

Exercise 10.2 We start from the 'continuous' inf-sup-stability estimate applied for $p_h \in Q_h \subset Q$:

$$\sup_{u\in V} \frac{(p_h, \nabla\cdot u)}{\|\varepsilon(u)\|} \geq \gamma\|p_h\|, \quad p_h \in Q_h\,.$$

With an H^1-stable local interpolant $\tilde{I}_h u \in V_h$, there holds

$$\begin{aligned}\frac{(p_h, \nabla\cdot u)}{\|\varepsilon(u)\|} &= \frac{(p_h, \nabla\cdot(u-\tilde{I}_h u)}{\|\varepsilon(u)\|} + \frac{(p_h, \nabla\cdot\tilde{I}_h u)}{\|\varepsilon(u)\|}\\ &= -\frac{(\nabla p_h, u-\tilde{I}_h u)}{\|\varepsilon(u)\|} + \frac{(p_h, \nabla\cdot\tilde{I}_h u)}{\|\varepsilon(\tilde{I}_h u)\|}\frac{\|\varepsilon(\tilde{I}_h u)\|}{\|\varepsilon(u)\|}\,.\end{aligned}$$

Noting the estimates

$$-\frac{(\nabla p_h, u-\tilde{I}_h u)}{\|\varepsilon(u)\|} \geq -c\sum_{K\in\mathbb{T}_h}\frac{\|\nabla p_h\|_K\|u-\tilde{I}_h u\|_K}{\|\nabla u\|} \geq -c\Big(\sum_{K\in\mathbb{T}_h} h_K^2\|\nabla p_h\|_K^2\Big)^{1/2},$$

and, by Korn inequality,

$$\frac{\|\varepsilon(\tilde{I}_h u)\|}{\|\varepsilon(u)\|} \leq c\,\frac{\|\nabla(\tilde{I}_h u)\|}{\|\nabla u\|} \leq c\,,$$

we obtain the inf-sup stability estimate

$$\sup_{u_h\in V_h}\frac{(p_h, \nabla\cdot u_h)}{\|\varepsilon(u_h)\|} + \Big(\sum_{K\in\mathbb{T}_h}\delta_K\|\nabla p_h\|_K^2\Big)^{1/2} \geq \gamma\,\|p_h\|, \quad p_h \in Q_h\,,$$

with $\delta_K = \alpha h_K^2$ and $\alpha > 0$ sufficiently large.

Chapter 11

Exercise 11.1 The surface-oriented form of the drag coefficient reads

$$c_{\text{drag}} = \frac{2}{\bar{U}^2 D} \int_S n^T (2\nu\tau - pI) e^{(1)} \, ds,$$

where $\tau = \frac{1}{2}(\nabla v + \nabla v^T)$. The divergence theorem states that $\int_\Omega \nabla\cdot f \, dx = \int_{\partial\Omega} n\cdot f \, do$. Therefore, we identify f with $(2\nu\tau - pI)\bar{e}^{(1)}$, where we extend $e^{(1)}$ away from S into the domain by $\bar{e}^{(1)}$. Thus,

$$c_{\text{drag}} = \frac{2}{\bar{U}^2 D} \int_{\partial\Omega} \nabla\cdot[(2\nu\tau - pI)\bar{e}^{(1)}] \, dx - \frac{2}{\bar{U}^2 D} \int_{\partial\Omega\setminus S} n^T (2\nu\tau - pI)\bar{e}^{(1)} \, ds.$$

Up to now, $\bar{e}^{(1)}$ is an arbitrary extension of $e^{(1)}$. In order to eliminate the second integral, we choose $\bar{e}^{(1)}$ such that it vanishes on $\partial\Omega\setminus S$. As long as we compute the drag coefficient of an object with finite distance to $\partial\Omega\setminus S$, $\bar{e}^{(1)}$ can be chosen to have finite gradient, thus avoiding problems with the definition of the domain integral.

Still, we do not want to compute $\nabla\cdot(2\nu\tau - pI)$ numerically since this involves second derivatives of the numerically computed solution. We therefore use that $\nabla\tau = \frac{1}{2}(\Delta v + \nabla\nabla\cdot v)$, and $\nabla\cdot(pI) = \nabla p$, and the state equation to rewrite $\nabla\cdot(2\nu\tau - pI) = -f + v\cdot\nabla v$, and thus obtain

$$c_{\text{drag}} = \frac{2}{\bar{U}^2 D} \int_{\partial\Omega} (v\cdot\nabla v - f)\cdot\bar{e}^{(1)} + (2\nu\tau - pI) : \nabla\bar{e}^{(1)} \, dx.$$

The computation for the lift coefficient follows the same procedure.

Exercise 11.2 For the given problem, the primal variational formulation uses the semilinear form

$$a(u)(\psi) = \nu(\nabla v, \nabla\psi^v) + (v\cdot\nabla v, \psi^v) - (p, \nabla\cdot\psi^v) - (v, \nabla\psi^p) - (f, \psi^v).$$

The dual problem is thus characterized by $a'(u)(\varphi, z) = J(\varphi)$, which reads in weak form:

$$\nu(\nabla\varphi^v, \nabla z^v) + (v\cdot\nabla\varphi^v, z^v) + (\varphi^v\cdot\nabla v, z^v) - (\varphi^p, \nabla\cdot z^v) - (\varphi^v, \nabla z^p) = J(\varphi).$$

In strong form, this leads to the equations

$$\begin{aligned} -\nu\Delta z^v - (\nabla\cdot v)z^v - v\cdot\nabla z^v + (\nabla v)z^v + \nabla z^p &= j, \\ \nabla\cdot z^v &= 0. \end{aligned}$$

Note that for the continuous dual problem, the second term in the first equation is actually zero, due to the incompressibility of v, but that it exists in the equation defining the discrete dual solution z_h. With the above, the residuals are

$$
\begin{aligned}
R^*_{h|K} &= j + \nu\Delta z^v_h + (\nabla\cdot v_h) z^v_h + v_h\cdot\nabla z^v_h - (\nabla v_h) z^v_h + \nabla z^p_h \\
r^*_{h|\Gamma} &= \begin{cases} \frac{1}{2}[\nu n\partial_n z^v_h + (v_h\cdot n) z^v_h - n z^p_h], & \text{if } \Gamma \not\subset \partial\Omega, \\ -\nu n\partial_n z^v_h - (v_h\cdot n) z^v_h + n z^p_h, & \text{if } \Gamma \subset \Gamma_{\text{out}}, \\ 0\,, & \text{otherwise.} \end{cases}
\end{aligned}
$$

Bibliography

[1] M. Ainsworth and J. T. Oden. A unified approach to a posteriori error estimation using element residual methods. *Numer. Math.*, 65:23–50, 1993.

[2] M. Ainsworth and J. T. Oden. A posteriori error estimation in finite element analysis. *Comput. Methods Appl. Mech. Eng.*, 142:1–88, 1997.

[3] M. Ainsworth and J. T. Oden. A posteriori error estimators for the Stokes and Oseen equations. *SIAM J. Numer. Anal.*, 34:228–245, 1997.

[4] J. P. Aubin. Behaviour of the error of the approximate solutions of boundary value problems for linear elliptic operators by Galerkin's and finite difference methods. *Ann. Scuola Morm. Sup. Pisa*, 21:599–637, 1967.

[5] I. Babuška and A. D. Miller. The post-processing approach in the finite element method, I: calculations of displacements, stresses and other higher derivatives of the displacements. *Int. J. Numer. Meth. Eng.*, 20:1085–1109, 1984.

[6] I. Babuška and A. D. Miller. The post-processing approach in the finite element method, II: the calculation of stress intensity factors. *Int. J. Numer. Meth. Eng.*, 20:1111–1129, 1984.

[7] I. Babuška and A. D. Miller. The post-processing approach in the finite element method, III: a posteriori error estimation and adaptive mesh selection. *Int. J. Numer. Meth. Eng.*, 20:2311–2324, 1984.

[8] I. Babuška and A. D. Miller. A feedback finite element method with a posteriori error estimation. *Comput. Methods Appl. Mech. Eng.*, 61:1–40, 1987.

[9] I. Babuška and W. C. Rheinboldt. Error estimates for adaptive finite element computations. *SIAM J. Numer. Anal.*, 15:736–754, 1978.

[10] I. Babuška and W. C. Rheinboldt. A posteriori error estimates for the finite element method. *Int. J. Numer. Meth. Eng.*, 12:1597–1615, 1978.

[11] I. Babuška and C. Schwab. A posteriori error estimation for hierarchic models of elliptic boundary value problems on thin domains. *SIAM J. Numer. Anal.*, 33:221–246, 1996.

[12] I. Babuška and T. Strouboulis. *The Finite Element Method and its Reliability.* Clarendon Press, Oxford, 2001.

[13] E. Backes. Gewichtete a posteriori Fehleranalyse bei der adaptiven Finite-Elemente-Methode: Ein Vergleich zwischen Residuen- und Bank-Weiser-Schätzer. Diploma thesis, Institute of Applied Mathematics, University of Heidelberg, 1997.

[14] W. Bangerth. Finite Element Approximation of the Acoustic Wave Equation: Error Control and Mesh Adaptation. Diploma thesis, Institute of Applied Mathematics, University of Heidelberg, 1998.

[15] W. Bangerth. Adaptive Finite Element Methods for the Identification of Distributed Parameters in Partial Differential Equations. Dissertation, Institute of Applied Mathematics, University of Heidelberg, 2002.

[16] W. Bangerth and R. Rannacher. Finite element approximation of the acoustic wave equation: Error control and mesh adaptation. *East–West J. Numer. Math.*, 7:263–282, 1999.

[17] R. E. Bank and A. Weiser. Some a posteriori error estimators for elliptic partial differential equations. *Math. Comp.*, 44:283–301, 1985.

[18] R. Becker. An Adaptive Finite Element Method for the Incompressible Navier–Stokes Equations on Time-Dependent Domains. Dissertation, Institute of Applied Mathematics, University of Heidelberg, 1995.

[19] R. Becker. An adaptive finite element method for the Stokes equations including control of the iteration error. *ENUMATH'97* (H. G. Bock *et al.*, eds), pp. 609–620, World Scientific, Singapore, 1998.

[20] R. Becker. An optimal-control approach to a posteriori error estimation for finite element discretizations of the Navier-Stokes equations. *East-West J. Numer. Math.*, 9:257–274, 2000.

[21] R. Becker. Mesh adaptation for stationary flow control. *J. Math. Fluid Mech.*, 3:317–341, 2001.

[22] R. Becker. Adaptive Finite Elements for Optimal Control Problems. Habilitation thesis, University of Heidelberg, 2001.

[23] R. Becker and M. Braack. Multigrid techniques for finite elements on locally refined meshes. *Numer. Linear Algebra Appl.*, 7:363–379, 2000.

[24] R. Becker and M. Braack. Solution of a stationary benchmark problem for natural convection with large temperature difference. *Int. J. Therm. Sci.*, 41:428–439, 2002.

[25] R. Becker, M. Braack, and R. Rannacher. Numerical simulation of laminar flames at low Mach number by adaptive finite elements. *Combust. Theory Modelling*, 3:503–534, 1999.

[26] R. Becker, M. Braack, R. Rannacher, and C. Waguet. Fast and reliable solution of the Navier–Stokes equations including chemistry. *Comput. Visual. Sci.*, 2:107–122, 1999.

[27] R. Becker, C. Johnson, and R. Rannacher. Adaptive error control for multigrid finite element methods. *Computing*, 55:271–288, 1995.

[28] R. Becker, H. Kapp, and R. Rannacher. Adaptive finite element methods for optimal control of partial differential equations: Basic concepts. *SIAM J. Control Optim.*, 39, 113–132, 2000.

[29] R. Becker and R. Rannacher. Weighted a posteriori error control in FE methods. Lecture at ENUMATH-95, Paris, Sept. 18-22, 1995, Preprint 96-01, SFB 359, University of Heidelberg, Proc. *ENUMATH'97* (H. G. Bock *et al.*, eds), pp. 621-637, World Scientific, Singapore, 1998.

[30] R. Becker and R. Rannacher. A feed-back approach to error control in finite element methods: Basic analysis and examples. *East-West J. Numer. Math.*, 4:237–264, 1996.

[31] R. Becker and R. Rannacher. An optimal control approach to error estimation and mesh adaptation in finite element methods. *Acta Numerica 2000* (A. Iserles, ed.), pp. 1-101, Cambridge University Press, 2001.

[32] R. Becker and B. Vexler. Adaptive finite element methods for parameter identification problems. Preprint 2002-20 (SFB 359), Universität Heidelberg, July 2002, *Numer. Math.*, submitted, 2002

[33] C. Bernardi, O. Bonnon, C. Langouët, and B. Métivet. Residual error indicators for linear problems: Extension to the Navier–Stokes equations. In Proc. *9th Int. Conf. Finite Elements in Fluids*, 1995.

[34] H. Blum, Q. Lin, and R. Rannacher. Asymptotic error expansion and Richardson extrapolation for linear finite elements. *Numer. Math.*, 49:11–37, 1986.

[35] H. Blum and F.-T. Suttmeier. An adaptive finite element discretization for a simplified Signorini problem. *Calcolo*, 37:65–77, 1999.

[36] H. Blum and F.-T. Suttmeier. Weighted error estimates for finite element solutions of variational inequalities. *Computing*, 65:119–134, 2000.

[37] K. Böttcher. Adaptive Schrittweitenkontrolle beim unstetigen Galerkin-Verfahren für gewöhnliche Differentialgleichungen. Diploma thesis, Institute of Applied Mathematics, University of Heidelberg, 1996.

[38] K. Böttcher and R. Rannacher. Adaptive error control in solving ordinary differential equations by the discontinuous Galerkin method. Technical Report Preprint 96-53, SFB 359, Universität Heidelberg, 1996.

[39] M. Braack. An Adaptive Finite Element Method for Reactive Flow Problems. Dissertation, Institute of Applied Mathematics, University of Heidelberg, 1998.

[40] M. Braack, R. Becker, and R. Rannacher. The dual-weighted residual method applied to three-dimensional flow problems. Computers & Fluids, Proc. 3. Int. Conf. on Appl. Math. for Industrial Flow Problems (AMIF), Lisbon, April 17-20, 2002, to appear.

[41] M. Braack and A. Ern. A posteriori control of modeling errors and discretization errors. Preprint 2002-13 (SFB 359), Universität Heidelberg, June 2002, SIAM J. Multiscale Modeling and Simulation, submitted, 2002.

[42] M. Braack and R. Rannacher. Adaptive finite element methods for low-Mach-number flows with chemical reactions. In H. Deconinck, editor, *30th Computational Fluid Dynamics, Lecture Series*, Vol. 1999-03, von Karman Institute for Fluid Dynamics, 1999.

[43] S. Brenner and R. L. Scott. *The Mathematical Theory of Finite Element Methods.* Springer, Berlin Heidelberg New York, 1994.

[44] G. F. Carey and J. T. Oden. *Finite Elements, Computational Aspects*, Vol. III. Prentice-Hall, 1984.

[45] C. Carstensen and R. Verfürth. Edge residuals dominate a posteriori error estimators for low-order finite element methods. *SIAM J. Numer. Anal.*, 36:1571–1587, 1999.

[46] P. G. Ciarlet. *Finite Element Methods for Elliptic Problems.* North-Holland, Amsterdam, 1978.

[47] R. Courant. Variational methods for the solution of problems of equilibrium and vibrations. *Bull. Amer. Math. Soc.*, 49:1–23, 1943.

[48] W. Dörfler and M. Rumpf. An adaptive strategy for elliptic problems including a posteriori controlled boundary approximation. *Math. Comp.*, 224:1361–1382, 1998.

[49] T. Dunne. Adaptive dual-gemischte Finite-Elemente-Verfahren. Diploma thesis, Institute of Applied Mathematics, University of Heidelberg, 2001.

[50] K. Eriksson, D. Estep, P. Hansbo, and C. Johnson. Introduction to adaptive methods for differential equations. *Acta Numerica 1995* (A. Iserles, ed.), pp. 105–158, Cambridge University Press, 1995.

[51] K. Eriksson and C. Johnson. An adaptive finite element method for linear elliptic problems. *Math. Comp.*, 50:361–383, 1988.

[52] K. Eriksson and C. Johnson. Adaptive finite element methods for parabolic problems, I: A linear model problem. *SIAM J. Numer. Anal.*, 28:43–77, 1991.

[53] K. Eriksson and C. Johnson. Adaptive streamline diffusion finite element methods for stationary convection-diffusion problems. *Math. Comp.*, 60:167–188, 1993.

[54] K. Eriksson and C. Johnson. Adaptive finite element methods for parabolic problems, II: Optimal error estimates in $L_\infty L_2$ and $L_\infty L_\infty$. *SIAM J. Numer. Anal.*, 32:706–740, 1995.

[55] K. Eriksson and C. Johnson. Adaptive finite element methods for parabolic problems, IV: Nonlinear problems. *SIAM J. Numer. Anal.*, 32:1729–1749, 1995.

[56] K. Eriksson and C. Johnson. Adaptive finite element methods for parabolic problems, V: Long-time integration. *SIAM J. Numer. Anal.*, 32:1750–1763, 1995.

[57] K. Eriksson, C. Johnson, and S. Larsson. Adaptive finite element methods for parabolic problems, VI: Analytic semigroups. *SIAM J. Numer. Anal.*, 35:1315–1325, 1998.

[58] D. Estep. A posteriori error bounds and global error control for approximation of ordinary differential equations. *SIAM J. Numer. Anal.*, 32:1–48, 1995.

[59] D. Estep and D. French. Global error control for the continuous Galerkin finite element method for ordinary differential equations. *Modél. Math. Anal. Numér.*, 28:815–852, 1994.

[60] J. Frehse and R. Rannacher. Eine L^1-Fehlerabschätzung für diskrete Grundlösungen in der Methode der finiten Elemente. Tagungsband Finite Elemente, *Bonn. Math. Schr.*, 89:92–114, 1976.

[61] C. Führer. Error Control in Finite Element Methods for Hyperbolic Problems. Dissertation, Institute of Applied Mathematics, University of Heidelberg, 1996.

[62] C. Führer and G. Kanschat. A posteriori error control in radiative transfer. *Computing*, 58:317–334, 1997.

[63] C. Führer and R. Rannacher. An adaptive streamline-diffusion finite element method for hyperbolic conservation laws. *East–West J. Numer. Math.*, 5:145–162, 1997.

[64] M. B. Giles. On adjoint equations for error analysis and optimal grid adaptation. In Frontiers of Computational Fluid Dynamics 1998 (D.A. Caughey and M.M. Hafez, eds), pp. 155-170. , World Scientific, 1998.

[65] M. B. Giles and N. A. Pierce. Adjoint error correction for integral outputs. Technical Report NA-01/18, Oxford University Computing Laboratory, 2001.

[66] M. B. Giles, M. G. Larsson, J. M. Levenstam, and E. Süli. Adaptive error control for finite element approximations of the lift and drag coefficients in viscous flow. NA-97/06, Oxford University Computing Laboratory, 1997.

[67] P. Hansbo. Three lectures on error estimation and adaptivity. *Adaptive Finite Elements in Linear and Nonlinear Solid and Structural Mechanics* (E. Stein, ed.), Vol. 416 of CISM Courses and Lectures, Springer, 2002, to appear.

[68] P. Hansbo and C. Johnson. Adaptive streamline diffusion finite element methods for compressible flow using conservative variables. *Comput. Methods Appl. Mech. Eng.*, 87:267–280, 1991.

[69] R. Hartmann. A posteriori Fehlerschätzung und adaptive Schrittweiten- und Ortsgittersteuerung bei Galerkin-Verfahren für die Wärmeleitungsgleichung. Diploma thesis, Institute of Applied Mathematics, University of Heidelberg, 1998.

[70] R. Hartmann. Adaptive FE-methods for conservation equations. In Proc. *8th International Conference on Hyperbolic Problems. Theory, Numerics, Applications (HYP2000)* (H. Freistühler and G. Warnecke, eds.), pp. 495–503, Int. Series of Numer. Math. 141, Birkhäuser, Basel, 2001.

[71] R. Hartmann. Adaptive Finite Element Methods for the Compressible Euler Equations. Dissertation, Institute of Applied Mathematics, University of Heidelberg, 2002.

[72] R. Hartmann and P. Houston. Adaptive discontinuous Galerkin finite element methods for nonlinear hyperbolic conservation laws. Preprint 2001-20 (SFB 359), Universität Heidelberg, *SIAM J. Sci. Comput.*, to appear.

[73] R. Hartmann and P. Houston. Adaptive discontinuous Galerkin finite element methods for the compressible Euler equations. Preprint 2001-41 (SFB 359), Universität Heidelberg, *J. Comput. Physics*, to appear.

[74] F.-K. Hebeker and R. Rannacher. An adaptive finite element method for unsteady convection-dominated flows with stiff source terms. *SIAM J. Sci. Comput.*, 21:799–818, 1999.

[75] J. Heywood, R. Rannacher, and S. Turek. Artificial boundaries and flux and pressure conditions for the incompressible Navier-Stokes equations. *Int. J. Comput. Fluid Mech.*, 22:325–352, 1996.

[76] V. Heuveline and C. Bertsch. *On multigrid methods for the eigenvalue computation of non-selfadjoint elliptic operators.* East-West J. Numer. Math. 8, 275–297 (2000).

[77] V. Heuveline and R. Rannacher. A posteriori error control for finite element approximations of elliptic eigenvalue problems. Preprint 2001-08 (SFB 359), University of Heidelberg, *J. Comput. Math. Appl.*, 15:107–138, 2001.

[78] V. Heuveline and R. Rannacher. Adaptive finite element discretization of eigenvalue problems in hydrodynamic stability theory. Preprint, SFB 359, Universität Heidelberg, March 2001.

[79] P. Houston, R. Rannacher, and E. Süli. A posteriori error analysis for stabilized finite element approximation of transport problems. *Comput. Methods Appl. Mech. Eng.*, 190:1483–1508, 2000.

[80] T. J. R. Hughes and A. N. Brooks. Streamline upwind/Petrov Galerkin formulations for convection dominated flows with particular emphasis on the incompressible Navier–Stokes equation. *Comput. Methods Appl. Mech. Eng.*, 32:199–259, 1982.

[81] T. J. R Hughes, G. R. Feijoo, L. Mazzei, and J.-B. Quincy. The variational multiscale method – a paradigm for computational mechanics. *Comput. Methods Appl. Mech. Eng.*, 166:3–24, 1998.

[82] T. J. R. Hughes, L. P. Franca, and M. Balestra. A new finite element formulation for computational fluid dynamics, V: Circumvent the Babuška–Brezzi condition: A stable Petrov–Galerkin formulation for the Stokes problem accommodating equal order interpolation. *Comput. Methods Appl. Mech. Eng.*, 59:89–99, 1986.

[83] C. Johnson. *Numerical Solution of Partial Differential Equations by the Finite Element Method.* Cambridge University Press, Cambridge, 1987.

[84] C. Johnson. Adaptive finite element methods for diffusion and convection problems. *Comput. Methods Appl. Mech. Eng.*, 82:301–322, 1990.

[85] C. Johnson. Adaptive finite element methods for the obstacle problem. *Math. Models Meth. Appl. Sci.*, 2:483–487, 1992.

[86] C. Johnson. Discontinuous Galerkin finite element methods for second order hyperbolic problems. *Comput. Methods Appl. Mech. Eng.*, 107:117–129, 1993.

[87] C. Johnson. A new paradigm for adaptive finite element methods. In J. Whiteman, ed., *Proc. MAFELAP 93.* John Wiley, 1993.

[88] C. Johnson and P. Hansbo. Adaptive finite element methods in computational mechanics. *Comput. Methods Appl. Mech. Eng.*, 101:143–181, 1992.

[89] C. Johnson and P. Hansbo. Adaptive finite element methods for small strain elasto-plasticity. *Finite Inelastic Deformations - Theory and Applications* (D. Besdo and E. Stein, eds), pp. 273–288, Springer, Berlin, 1992.

[90] C. Johnson and R. Rannacher. On error control in CFD. Proc. Int. Workshop *Numerical Methods for the Navier-Stokes Equations* (F.-K. Hebeker *et al.*, eds), pp. 133–144, *vol. 47 of Notes Num. Fluid Mech*, Vieweg, Braunschweig, 1994.

[91] C. Johnson, R. Rannacher, and M. Boman. Numerics and hydrodynamic stability: Towards error control in CFD. *SIAM J. Numer. Anal.*, 32:1058–1079, 1995.

[92] C. Johnson and A. Szepessy. Adaptive finite element methods for conservation laws based on a posteriori error estimates. *Comm. Pure Appl. Math.*, 48:199–234, 1995.

[93] G. Kanschat. Parallel and Adaptive Galerkin Methods for Radiative Transfer Problems. Dissertation, Institute of Applied Mathematics, University of Heidelberg, 1996.

[94] G. Kanschat. Solution of multi-dimensional radiative transfer problems on parallel computers. *Parallel Solution of Partial Differential Equations* (P. Bjørstad and M. Luskin, eds), pp. 85–96, vol. 120 of *IMA Volumes in Mathematics and its Applications*, New York, 2000. Springer.

[95] G. Kanschat and R. Rannacher. Local error analysis of the interior penalty discontinuous Galerkin method. Preprint, Universität Heidelberg, 2002.

[96] H. Kapp. Adaptive Finite Element Methods for Optimization in Partial Differential Equations. Dissertation, Institute of Applied Mathematics, University of Heidelberg, 2000.

[97] G. Kunert. An a posteriori residual error estimator for the finite element method on anisotropic tetrahedral meshes. *Numer. Math.*, 86:471–490, 2000.

[98] G. Kunert. A posteriori L_2 error estimation on anisotropic tetrahedral finite element meshes. *IMA J. Numer. Anal.*, 21:503–523, 2001.

[99] G. Kunert. Edge residuals dominate a posteriori error estimates for linear finite element methods on anisotropic triangular and tetrahedral meshes. *Numer. Math.*, 86:283–303, 2000.

[100] P. Ladeveze and D. Leguillon. Error estimate procedure in the finite element method and applications. *SIAM J. Numer. Anal.*, 20:485–509, 1983.

[101] M. G. Larson. A posteriori and a priori error estimates for finite element approximations of selfadjoint eigenvalue problems. *SIAM J. Numer. Anal.*, 38:608–625, 2000.

[102] M. G. Larson and A. J. Niklasson. Adaptive multilevel finite element approximations of semilinear elliptic boundary value problems. *Numer. Math.*, 84:249–274, 1999.

[103] W. Liu and N. Yan. A posteriori error estimates for some model boundary control problems. *J. Comput. Appl- Math.*, 120:159–173, 2000.

[104] W. Liu and N. Yan. Local a posteriori error estimates for convex boundary control problems. Preprint, University of Kent, 2002.

[105] L. Machiels, A. T. Patera, and J. Peraire. Output bound approximation for partial differential equations; application to the incompressible Navier-Stokes equations. In S. Biringen, editor, *Industrial and Environmental Applications of Direct and Large Eddy Numerical Simulation.* Springer, Berlin Heidelberg New York, 1998.

[106] L. Machiels, J. Peraire, and A. T. Patera. A posteriori finite element output bounds for the incompressible Navier-Stokes equations: application to a natural convection problem. Technical Report 99-4, MIT FML, 1999.

[107] J. Nitsche. Ein Kriterium für die Quasi-Optimalität des Ritzschen Verfahrens. *Numer. Math.*, 11:346–348, 1968.

[108] C. Nystedt. A priori and a posteriori error estimates and adaptive finite element methods for a model eigenvalue problem. Technical Report Preprint NO 1995-05, Department of Mathematics, Chalmers University of Technology, 1995.

[109] J. T. Oden. Finite elements: an introduction. In *Handbook of Numerical Mathematics, Vol. II, Finite Element Methods (Part 1)* (P.G. Ciarlet and J.L. Lions, eds), pp. 3–15, North-Holland, Amsterdam. 1991.

[110] J. T. Oden and S. Prudhomme. On goal-oriented error estimation for elliptic problems: Application to the control of pointwise errors. *Comput. Methods Appl. Mech. Eng.*, 176:313–331, 1999.

[111] J. T. Oden and S. Prudhomme. Estimation of modeling error in computational mechanics. Preprint, TICAM, The University of Texas at Austin, 2002.

[112] J. T. Oden, W. Wu, and M. Ainsworth. An a posteriori error estimate for finite element approximations of the Navier–Stokes equations. *Comput. Methods Appl. Mech. Eng.*, 111:185–202, 1993.

[113] M. Paraschivoiu and A. T. Patera. Hierarchical duality approach to bounds for the outputs of partial differential equations. *Comput. Methods Appl. Mech. Eng.*, 158:389–407, 1998.

[114] R. Rannacher. Error control in finite element computations. *Proc. Summer School Error Control and Adaptivity in Scientific Computing* (H. Bulgak and C. Zenger, eds), pp. 247–278. Kluwer Academic Publishers, 1998.

[115] R. Rannacher. A posteriori error estimation in least-squares stabilized finite element schemes. *Comput. Methods Appl. Mech. Eng.*, 166:99–114, 1998.

[116] R. Rannacher. *Finite element methods for the incompressible Navier-Stokes equations.* Fundamental Directions in Mathematical Fluid Mechanics (G. P. Galdi, J. Heywood, R. Rannacher, eds), pp. 191–293, Birkhäuser, Basel-Boston-Berlin, 2000.

[117] R. Rannacher. Duality techniques for error estimation and mesh adaptation in finite element methods. *Adaptive Finite Elements in Linear and Nonlinear Solid and Structural Mechanics* (E. Stein, ed.), vol. 416 of CISM Courses and Lectures, Springer, 2002.

[118] R. Rannacher and F.-T. Suttmeier. A feed-back approach to error control in finite element methods: Application to linear elasticity. *Computational Mechanics*, 19:434–446, 1997.

[119] R. Rannacher and F.-T. Suttmeier. A posteriori error control in finite element methods via duality techniques: Application to perfect plasticity. *Computational Mechanics*, 21:123–133, 1998.

[120] R. Rannacher and F.-T. Suttmeier. A posteriori error estimation and mesh adaptation for finite element models in elasto-plasticity. *Comput. Methods Appl. Mech. Eng.*, 176:333–361, 1999.

[121] R. Rannacher and F.-T. Suttmeier. Error estimation and adaptive mesh design for FE models in elasto-plasticity. *Error-Controlled Adaptive FEMs in Solid Mechanics* (E. Stein, ed.), John Wiley, to appear.

[122] S. Richling, E. Meinköhn, N. Kryzhevoi, and G. Kanschat. Radiative transfer with finite elements I. Basic method and tests. *A&A*, 380:776–788, 2001.

[123] T. Richter. Funktionalorientierte Gitteroptimierung bei der Finite-Elemente-Approximation elliptischer Differentialgleichungen. Diploma thesis, Institute of Applied Mathematics, University of Heidelberg, 2001.

[124] M. Schäfer and S. Turek. Benchmark computations of laminar flow around a cylinder. (With support by F. Durst, E. Krause and R. Rannacher). *Flow Simulation with High-Performance Computers II (E. H. Hirschel, ed.), pp. 547-566, DFG priority research program results 1993-1995*, vol. 52 of Notes Numer. Fluid Mech., Vieweg, Wiesbaden, 1996.

[125] L. R. Scott and S. Zhang. Finite element interpolation of nonsmooth functions satisfying boundary conditions. *Math. Comp.*, 54:483–493, 1990.

[126] K. Siebert. An a posteriori error estimator for anisotropic refinement. *Numer. Math.*, 73:373–398, 1996.

[127] E. Stein and S. Ohnimus. Coupled model- and solution-adaptivity in the finite-element method. *Comput. Methods Appl. Mech. Eng.*, 150:327–350, 1997.

[128] F.-T. Suttmeier. Adaptive Finite Element Approximation of Problems in Elasto-Plasticity Theory. Dissertation, Institute of Applied Mathematics, University of Heidelberg, 1996.

[129] F.-T. Suttmeier. An adaptive displacement/pressure finite element scheme for treating incompressibility effects in elasto-plastic materials. *Numer. Meth. Part. Diff. Equ.*, 17:369–382, 2001.

[130] R. Verfürth. A posteriori error estimates for nonlinear problems. *Numerical Methods for the Navier-Stokes Equations* (F.-K. Hebeker et al., eds), pp. 288–297, vol. 47 of *Notes Numer. Fluid Mech.*, Vieweg, Braunschweig, 1993.

[131] R. Verfürth. A posteriori error estimates for nonlinear problems. Finite element discretization of elliptic equations. *Math. Comp.*, 62:445–475, 1994.

[132] R. Verfürth. *A Review of A Posteriori Error Estimation and Adaptive Mesh-Refinement Techniques.* Wiley/Teubner, New York Stuttgart, 1996.

[133] R. Verfürth. A posteriori error estimation techniques for nonlinear elliptic and parabolic pde's. *Rev. Eur. Élém. Finis*, 9:377–402, 2000.

[134] B. Vexler. A posteriori Fehlerschätzung und Gitteradaption bei Finite-Elemente-Approximationen nichtlinearer elliptischer Differentialgleichungen. Diploma thesis, Institute of Applied Mathematics, University of Heidelberg, 2000.

[135] C. Waguet. Adaptive Finite Element Computation of Chemical Flow Reactors. Dissertation, Institute of Applied Mathematics, University of Heidelberg, 2000.

[136] R. Zamni. Integrationsfehleranalyse bei der adaptiven Finite-Elemente-Methode. Diploma thesis, Institute of Applied Mathematics, University of Heidelberg, 2001.

[137] O. C. Zienkiewicz and J. Z. Zhu. A simple error estimator and adaptive procedure for practical engineering analysis. *Int. J. Numer. Meth. Eng.*, 24, 1987.

[138] M. Zlámal. On the finite element method. *Numer. Math.*, 12:394–409, 1968.

Index